S. Reyes Cortes, N.C. Hawkes, P. Lotte, C. Fenzi, B.C. Stratton,
J. Hobirk, R. De Angelis, F. Orsitto and C.A.F. Varandas

# Measurement of the Plasma Radial Electric Field by the Motional Stark Effect Diagnostic on JET Plasmas

# Measurement of the Plasma Radial Electric Field by the Motional Stark Effect Diagnostic on JET Plasmas

S. Reyes Cortes, N.C. Hawkes[1], P. Lotte[2], C. Fenzi[2], B.C. Stratton[3],
J. Hobirk[4], R. De Angelis[5], F. Orsitto[5], C.A.F. Varandas[6]
and contributors to the EFDA-JET workprogramme*

*Associação EURATOM/IST, Departamento de Física, Universidade da Beira Interior,
6201-001 Covilhã, Portugal*
*[1]Euratom/UKAEA Fusion Association, Culham Science Centre, Abingdon, OX14 3DB, UK*
*[2]Association Euratom/CEA, CEA-Cadarache, F-13108, St.Paul les Durance, France*
*[3]Princeton Plasma Physics Laboratory, PO Box451, Princeton, NJ 08543, USA*
*[4]Max-Planck-Institut fur Plasmaphysik, Euratom Association, Boltzmannstr. 2, Garching, Germany*
*[5]Association Euratom-ENEA sulla Fusione, CRE Frascati, Roma, Italy*
*[6]Associação EURATOM/IST, Centro de Fusão Nuclear, Av. Rovisco Pais, 1049-001 Lisboa, Portugal*
*\* See annex of J. Pamela et al, "Overview of Recent JET Results and Future Perspectives",
Fusion Energy 2000 (Proc. 18th International Conference on Controlled Fusion and Plasma Physics,
Sorrento, 2000), IAEA, Vienna (2001)*

**ABSTRACT**

The radial electric field gradient or the E x B flow shear has been pointed out as the underlying mechanism for turbulence suppression, responsible for an internal transport barrier formation in advanced tokamak scenarios. A comprehensive study on these subjects requires a direct measurement of the plasma radial electric field $E_r$. The poloidal component of the magnetic field is assessed by the Motional Stark Effect (MSE) polarimeter, which is currently a standard diagnostic in fusion devices, allowing a local and non perturbative measurement of the magnetic pitch angle. A precise measure to the state of polarisation of the Stark components gives the information on the direction of the magnetic field. Due to the particular orientation of the Lorentz component, that is nearly perpendicular to $E_r$, the MSE diagnostic is very sensitive to the plasma intrinsic radial electric field. This paper describes a technique to measure $E_r$ involving the change of the polarisation angle of the MSE emission, by using two beam injectors at different energies, firing sequentially. Experimental results for the low $E_r$ case, i.e. with very little plasma rotation, showing the ability of the MSE to perform this measurement, will be presented. This is the first time that evidence of a direct measurement of the plasma $E_r$ is reported from JET.

## 1. INTRODUCTION

The safety factor or its inverse the so-called rotational transform plays a role in the equilibrium and stability of magnetically confined plasmas. The accurate measure of these quantities is needed in studies involving optimised shear scenarios, transport phenomena, MHD stability and confinement. The Motional Stark Effect (MSE) diagnostic was first developed [1, 2] aiming at active control of the q profiles, and consequently the current density distribution j(r), in auxiliary heated discharges using RF, heating beams and other methods appropriate to the current generation of fusion devices. The MSE system relies in the Stark splitting of the $D_\alpha$ line excited by collisions between the neutrals particles, injected by the heating beams, and plasma ions. As the neutrals passes through the magnetic field they experience the Lorentz field given by

$$\vec{E}_{tot} = \vec{v} \times \vec{B} \qquad\qquad (1)$$

in the rest frame of the neutral atom. This emission has two orthogonal polarised components allowed, the $\pi$ emission for $\Delta m = 0$ and $\sigma$ emission for $\Delta m = \pm 1$. When viewed in a direction perpendicular to $E_{tot}$, the polarisation directions of these components are parallel or perpendicular, respectively, to the motional electric field. By measuring the polarisation angle of one of these components, it is possible to determine the safety factor. In general j(r) must be calculated using an equilibrium reconstruction code such EFIT [3], and using the MSE data as a constraint, to solve numerically the Grad- Shafranov equation. In section 2 of this article the MSE system, currently a routine diagnostic at JET, will be reviewed.

The detailed knowledge of the profile of the plasma radial electric field $E_r$ and particularly its gradient or flow shear $\omega'_{E\,x\,B}$ has been recognised as a major factor involved in theories of turbulence

suppression and stabilisation of MHD activity. Also evidence of its role in enhanced confinement regimes have been reported [4].

In magnetically confined plasma $E_r$ is determined by the radial force balance equation

$$\nabla_r P_i = n_i e_i \, (\vec{E_r} + \vec{v_i} \times \vec{B}) \tag{2}$$

where the subscript $i$ stands for each plasma species, being $e_i$, $n_i$, $p_i$ and $v_i$ the charge, density, pressure and fluid velocity respectively, evaluated on the flux surface for each species. It should be noted that the quantity $E_r$ is not a flux function, but the quantity $E_r/RB_\theta$ is. Equation (3) can be simplified, adopting a cylindrical coordinate system (R, $\varphi$, z) to give

$$E_r = (n_i e_i)^{-1} \nabla_r P_i - v_{\theta i} B_\varphi + v_{\varphi i} B_\theta \tag{3}$$

From the last equation we can expect large electric fields either when the toroidal momentum is high or the pressure gradients are large. In section 3 we will discuss the interference of the electric field with the MSE measurements. The poloidal velocity is not measured directly in the core at JET. So this term is usually computed from the neoclassical theory, where a code like TRANSP can predict that this term is small (10-20%) compared with the toroidal term, so the accuracy of the calculated vq is not crucial in the estimation of $E_r$. The toroidal velocity is the dominant term at JET and can be obtained from charge exchange recombination spectroscopy.

Section 4 will provide a brief introduction in the fundamentals of the techniques for measuring the plasma radial electric field by the MSE system.

## 2. THE MOTIONAL STARK EFFECT DIAGNOSTIC AT JET

A motional Stark effect diagnostic is currently installed at JET [5, 6]. Neutral heating deuterium beam atoms are injected with velocities of $3 \times 10^6$ ms$^{-1}$. Collisions with plasma ions cause excitation and emission of the $D_\alpha$ line at 656.3nm. The beam atoms as crosses the JET plasma magnetic fields of the order of few Tesla, they experience the strong Lorentz field of nearly 5 MVm$^{-1}$ causing Stark splitting of emitted lines. This emission is also Doppler shifted. As mentioned above, this emission has two polarised components $\pi$ and $\sigma$. Precise knowledge of the direction of any of these two components allows measuring the direction of the plasma magnetic field. The polarised light emitted from the plasma is collected by an imaging optical system, made from low Verdet constant glass to avoid Faraday rotation in the transmission optics. The collected light is conveyed to the polarimeter consisting of two PhotoElestic Modulators (PEMs) in tandem and a linear polariser that encode in amplitude the phase of the polarised light coming from the plasma. The two PEMs have their fast axes oriented at 45$^o$ relative to each other, and the linear polarizer is oriented at 22.5$^o$ of each. The modulated light is transported by an optical fibre link to a remotely located detection system. The detection system consists of a set of 25 interference filters spectrometers, each one corresponding to a line of sight of the MSE system, observing the Stark feature of the $D_\alpha$ emission. Each interference filter or MSE channel is optically coupled to an avalanche photodiode. The modulated signals are

carried to a data acquisition system where they are digitised and the Fourier components at the first and second harmonics of the PEMs frequencies extracted. The interference filters having a bandpass of 0.4nm spectrally resolve the Stark components. At this point it should be noted that the presence of energy components at one half and one third of the full energy (Fig. 2) significantly increase the complexity of the Stark spectrum.

The JET neutral heating system consists of two banks with normal and tangential directions (Fig. 1). This causes additional complexity in the observed spectrum, as light with different polarisation and different Doppler shifts interferes with the MSE injector or PINI 1 (Positive Ion Neutral Injector). This problem was partially solved tuning the diagnostic to the emission of an injector from the tangential bank, which has the largest Doppler shift, isolating thisemission from normal bank injectors emission. The longer wavelength +π from injector 1, was choose to avoid interference of tangential bank injectors. The experimental Stark spectrum is represented in figure 3 (right), where can be noticed two carbon lines very close to the +π line and in some cases even superimposed to these carbon lines (edge channels 1 to 8). This causes an extra complexity in analysing results. Currently these problems are solved by increasing the energy of the MSE neutral injector up to 130keV, shifting the +π line in nearly 3nm.

Further analysis in interpreting the data involves the use of Stokes polarimetry. Where the stokes tetravector [I, M, C, R] encodes the pitch angle and degree of polarisation. Here I represent the total intensity M and C the degree and orientation of the linear polarised component. Finally, R represents the degree of circular polarisation. The input and output Stokes vectors are related with the mirror and relay optics through the Muller matricies describing the optical system [7].

## 3. INCLUDING THE $E_r$ EFFECT IN THE MSE MEASUREMENTS

A relationship between the measured pitch angle and the motional electric field [8] can be derived, by considering a new reference system ($e_x'$, $e_y'$, $e_z'$) linked to the MSE line of sight where ex' is coincident with the diagnostic line of sight, such that

$$\tan \gamma_m = \frac{E_y'}{E_z'} = \frac{E_{tot} \cdot \vec{e}_y'}{E_{tot} \cdot \vec{e}_z'} \tag{4}$$

In the simplest case $E_{tot}$ is described by equation (1) corresponding to the Lorentz field. The relationship between the measured pitch angle can be written in a parameterised form

$$\tan \gamma_m = \frac{E_y'}{E_z'} = \frac{B_v A_0 + B_R A_1 + B_T A_2}{B_v A_3 + B_R A_4 + B_T A_5} \tag{5}$$

where the magnetic components $B_v$ and $B_R$ have been introduced taking into account the more general case of a non coplanar geometry with the magnetic axis slightly shifted. The $A_i$ coefficients includes the geometrical factors (not shown) involving the angles $\alpha$ and $\Omega$ (see Fig. 3) for any general geometry. The coefficients also include factors with angles $\delta$ and $\theta$ (not shown) corresponding

to the inclinations of the neutral beams and lines of sight respectively. In the JET geometry the quantities $B_R$, $\delta$ and $\theta$ are very small near the midplane. Hence equation (5) can be simplified leading to the standard expression for the measured pitch angle

$$\tan \gamma_m = \tan \gamma \; \frac{\cos (\alpha + \Omega)}{\sin \alpha} \qquad (6)$$

The local magnetic pitch angle is equal to the measured pitch angle corrected by a geometric factor.

Previous analysis of the MSE data did not take into account the influence of the plasma radial electric field. At that time was believed that it should be very little and would not perturb the MSE measurements. Clearly, this not the case when large toroidal rotation velocities and pressure gradients are expected, as is the case in new improved high performance scenarios. This sensitivity of the MSE to $E_r$ was first noticed by Zarnstorff and coworkers [9]. Hence it is necessary to include the radial electric field in equation (1)

$$\vec{E}_{tot} = \vec{v} \times \vec{B} + \vec{E}_r \qquad (7)$$

Here the direction of $E_r$ is perpendicular to the flux surface, and equation (6) is modified to include an extra coefficient $A_6$, defined as

$$A_6 \frac{\cos \Omega \cos \delta \cos \theta}{V_b} \qquad (8)$$

where $v_b$ is the neutral beam velocity. Considering $B_R$, $\delta$ and $\theta$ very small on the JET midplane, equation (5) can be simplified to include the effect of the plasma radial electric field

$$\tan \gamma_m \; - \; \frac{B_v A_0 + E_r A_6}{B_T A_5} \qquad (9)$$

or

$$\tan \gamma_m \approx \frac{V_b B_V \cos(\alpha + \Omega) + E_r \cos \Omega}{V_b B_V \sin \alpha} \qquad (10)$$

## 4. MEASURING TECHNIQUE AND RESULTS

The significance of equation (10) is two fold. From one point of view makes clear the effective interference of $E_r$ on the measured pitch angle. This sensitivity of the MSE system to $E_r$ is due to the particular orientation of this vector that is almost perpendicular to the Lorentz field. This effect is illustrated in Fig. 3, (right).

The way to correct this effect in the measured pitch angle is to compute the radial electric field from the radial force balance equation (3). Using charge exchange spectroscopy (CXS) data to measure the toroidal rotation, and correct the measured values through equation (10). The practical effect of this correction is to decrease the core values of the qprofiles typically by 10% to 40% (Fig. 4, left).

4

From another point of view, equation (10) is clearly non linear in $\gamma = B_V / B_T$ an $E_r$ or $\gamma_m = f(\gamma, E_r)$. The optimal method to separate equation (10) should take advantage of the use of different angles at the same measurement location [8]. However this technique would imply an extra MSE system, thus precluding to be used at JET.

Another approach to this problem is to exploit different neutral beam injector energies, leading to different $v_b$ values for the same measurement. This technique has been used elsewhere [10, 11], but using a single beam injector, with the MSE channels tuned to the full and half energy fractions of the beam. However is not clear yet whether this approach works in large size devices due to the strong attenuation of the half energy component. In our case we choose two different injectors firing sequentially at different energies. This is the beam switching technique. Figure (4, right) shows the simulated Stark spectrum for PIN I 1 (130keV) and PIN I 7 (80keV). Vertical bars limits schematically the filter bandpass of a double cavity interference filter. Using equation (9) for each injector we can derive an expression to be used in the measure of $E_r$

$$ E_r = \frac{1}{C} \, B_T \, \Delta\tan \gamma_m \tag{11} $$

where the constant C embody the $A_i$ geometric coefficients including $A_6$ in equation (8). Equation (11) has been used to perform a check to the sensitivity of the MSE system to several PINI configurations using CXS data. The results presented in figure (6) have shown that the most suitable configuration is PINI 1/PINI 7 firing at 130keV and 80keV respectively. The experimental setup for the measurement is presented in Fig. 6, showing schematically PINI 1 and PINI 7 firing sequentially with a 0.1s duty cycle. Missing data, that is data points when each PIN I was not firing were interpolated from neighbouring blips. Half of the channels were tuned to the $+\pi$ lines from PINI 1 and the other half to the $+\pi$ emission from PINI 7. During the experiment the plasma $E_r$ was altered by increasing the toroidal velocity, using the torque of all the injectors available from octant 4. At the same time the MSE time window was splited, aiming to measure the electric field during the spin down of the plasma rotation. Results of the measurement are illustrated in Fig 7. In Fig. 7 (a) shows PINI 1 and PINI 7 firing sequentially, also can be seen the total power with all the available injectors from octant 4. Figure 7(b) represent MSE signals from two adjacent channels tuned to the $+\pi$ lines from PINI 1 and PINI 7 respectively. Figure 7(c) shows the $E_r$ time evolution as given by equation (11).

The time evolution of $E_r$ tracked for several MSE channels, makes possible to determine the radial profile of $E_r$ (Fig. 8). From here we can notice a global decrease of $E_r$ after the high power phase. A good agreement between the position of the magnetic axis (~ channel 17 or 18 at 3.128m and 3.079m) and an expected near zero electric field can be observed.


## 5. CONCLUSIONS

Experimental evidence of a direct measurement of the plasma radial electric field has been demonstrated, at JET tokamak using the beam switching technique. This technique could be an

alternative (or complement) to other methods reported from DIII-D [7]. Additional work is planned to use the technique in advanced tokamak regimes at JET.

**REFERENCES**

[1]. F.M. Levinton et al., Phys.Rev.Lett., 63, 2060 (1989)

[2]. D.Wroblewsky et al, Phys.Rev.Lett., 61, 3552 (1990)

[3]. L.Lao et al., Nucl.Fusion, 25, 1611 (1985)

[4]. N.C.Hawkes et al., Proc.27th EPS on Cont. Fusion & Plasma Phys. Budapest, Hungary (2000)

[5]. N.C. Hawkes et al., Rev.Sci. Instrum., 70, 894 (1999)

[6]. B.C. Stratton et al., Rev.Sci.Instrum., 70, 898 (1999)

[7]. N.C. Hawkes, JET Internal Report, JET-R(96)10 (Unpublished)

[8]. B.W. Rice et al., Rev.Sci.Instrum., 70, 815 (1999)

[9]. M.C. Zarnstoff et al., Phys.Plasmas 4, 1097 (1997)

[10]. J.Hobirk et al., Proc.27th EPS on Contr. Fusion and Plasma Physics Budapest, Hungary (2000)

[11]. F.M.Levinton et al., Phys.Rev.Lett., 80, 4887 (1998)
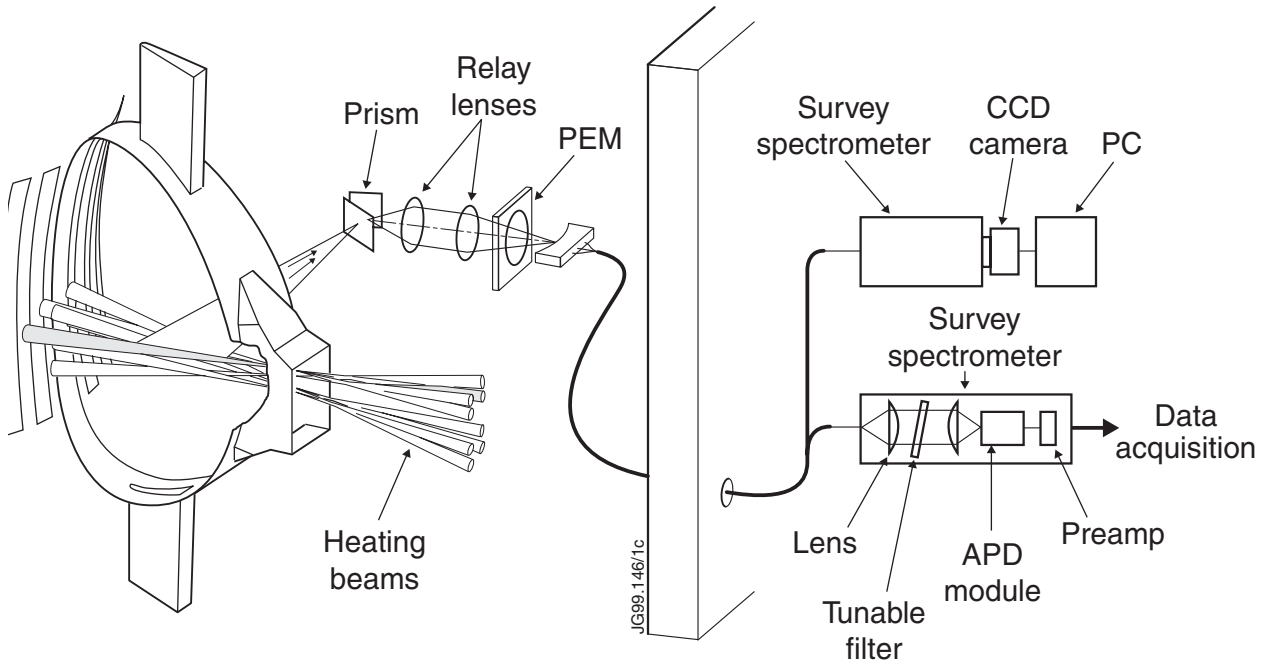
*Figure 1: Poloidal and toroidal projections of JET tokamak showing the neutral beams tracks (left) and the MSE lines of sight (right).*



*Figure 2: Polodial and torodial projections of JET tokamak showing the neutral beams tracks (left) and the MSE lines of sight (right).*
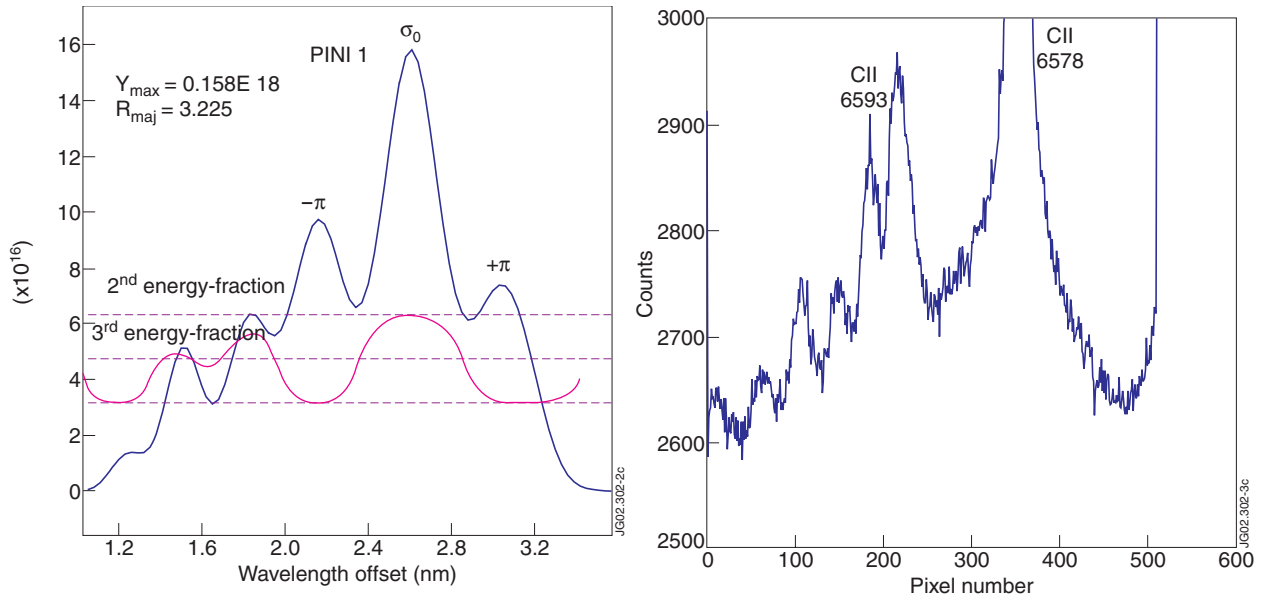
7

*Figure 3: Simulated stark spectrum (right) shows the relevant emission lines and the half and the third energy components (80 keV, 3.25m) The units correspond to the seperation from the rest $D_\alpha$ line. Experimental spectrum (left) showing the edge carbon lines overlapping the stark spectrum.*
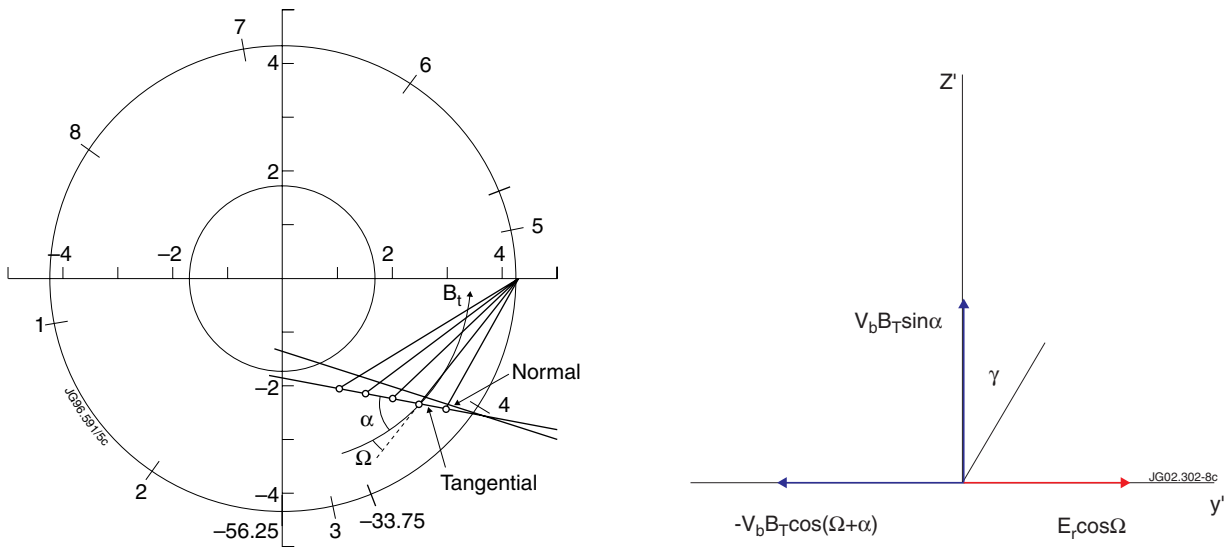


*Figure 4: MSE geometry (left) and Er interference (right).*
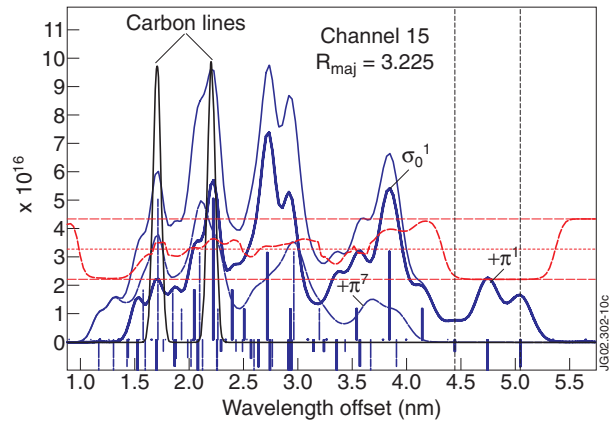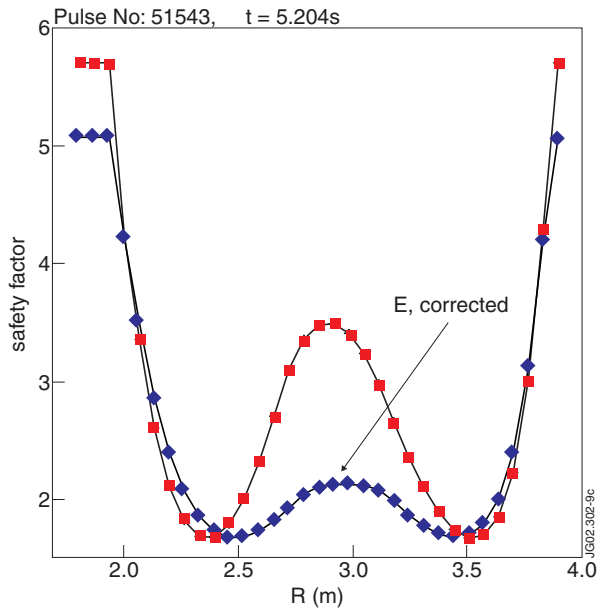
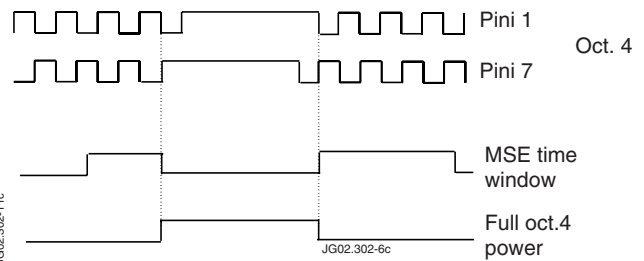*Figure 5: Effect of $E_r$ on the reconstructed q-profile (left). Simulated spectrum (right) for PINI 1 (MSE measurement, 130 keV) and PINI 7 (80 keV).*
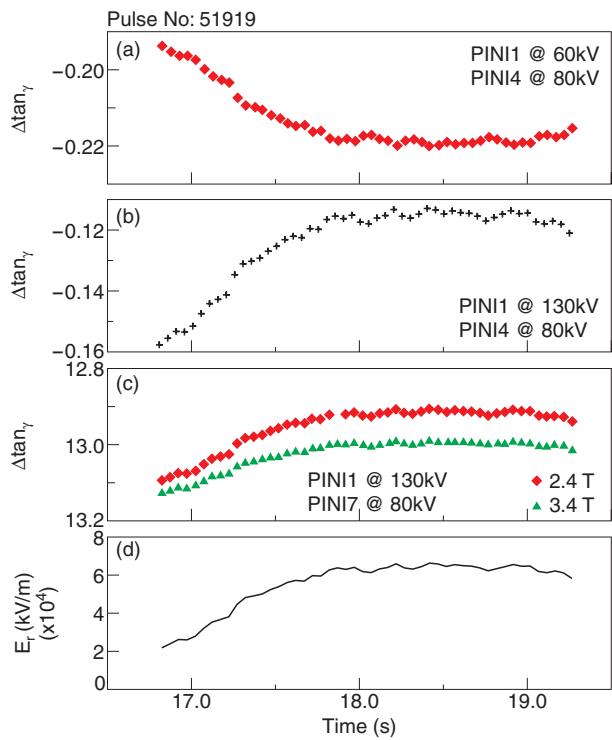




*Figure 5: a), low sensitivity for the PINI 1/PINI 4 configuration (~0.01°/20 kVm⁻¹). b) improved sensitivity for the PINI1/PINI7 configuration (~0.1°/20 kVm⁻¹). c) Strong dependence of the sensitivity on BT d) $E_r$ calculated from CXS data.*

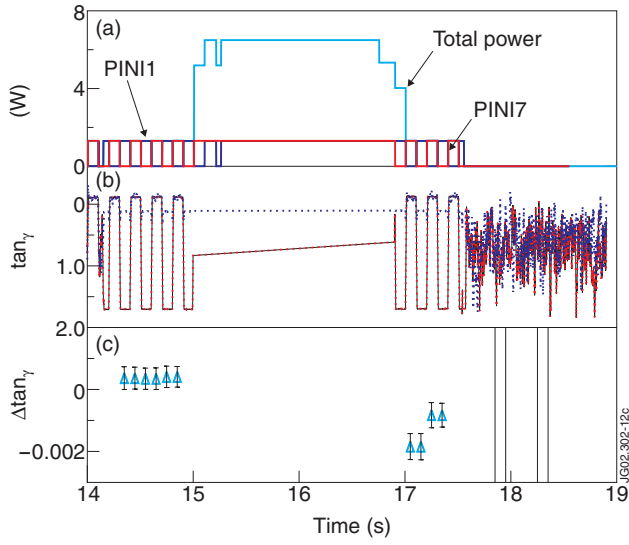*Figure 6: Experimental setup for $E_r$ measurement.*

*Figure 8: a) neutral beam powers. b) MSE signals for channels 10 and 11 c) time evolution of $E_r$ as seen by channel 11.*
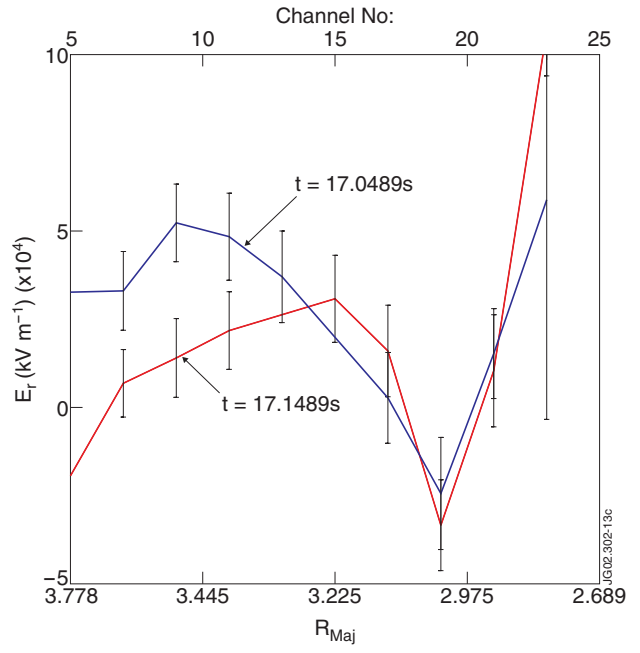


*Figure 9: Radial profile of $E_r$.*